Finally, just as C_{60} fullerenes yielded fullerene tubes, WAu_{12} could lead to various (now filled) extended structures. Judging from the short W–Au distances, they might have substantial mechanical strength. The mutual coupling of such structures by chemical bonds[14] or by the ionic interactions already mentioned is a further possibility.

Summarizing, if these triply stabilized, icosahedral 5d metal clusters could be made, they might provide a new structural "principle" in gold chemistry.

Computational Methods

The reported calculations have been performed at the Hartree – Fock (HF), second-order Møller – Plesset (MP2), or B3LYP DFT level. The MP2 calculations were performed within the resolution-of-identity (RI) approximation.[15, 16] The core electrons were replaced with quasirelativistic pseudopotentials[17] resulting in 14 and 19 valence electrons for W and Au, respectively. The corresponding valence basis sets are of (7s6p5d)/[6s3p3d] quality and labelled as TZVP. The TZVP was further extended by one f function for both W and Au[18] (TZVPP). The largest basis set, TZVPP + f(Au), was obtained by replacing the single f function in TZVPP by two f functions on gold.[19] All calculations have been done with the TURBOMOLE program package.[20]

Received: December 17, 2001 [Z18400]

[1] D. T. Thompson, *Gold Bull. (London)* **2001**, *34*, 56.
[2] D. A. H. Cunningham, W. Vogel, H. Kageyama, S. Tsubota, M. Haruta, *J. Catal.* **1998**, *177*, 1.
[3] P. Pyykkö, N. Runeberg, *J. Chem. Soc. Chem. Commun.* **1993**, 1812.
[4] P. Pyykkö, T. Tamm, *Organometallics* **1998**, *17*, 4842.
[5] P. Pyykkö, *Chem. Rev.* **1988**, *88*, 563. For the latest benchmarks for relativistic effects on gold atoms, molecules, and solids, see P. Pyykkö, *Angew. Chem.* **2002**, submitted.
[6] D. M. P. Mingos, *J. Chem. Soc. Dalton Trans.* **1976**, 1163. Note that only the bonding orbitals of a_g and t_{1u} symmetry were quoted. The HOMO was wrongly supposed to be t_{1u}. The present bonding h_g orbital was hidden in a 13($5d^{10}$) core band.
[7] C. E. Briant, B. R. C. Theobald, J. W. White, L. K. Bell, D. M. P. Mingos, A. J. Welch, *J. Chem. Soc. Chem. Commun.* **1981**, 201.
[8] R. Arratia-Perez, L. Hernández-Acevedo, *Chem. Phys. Lett.* **1999**, *303*, 641, and references therein.
[9] K. Michaelian, N. Rendón, I. L. Garzón, *Phys. Rev. B* **1999**, *60*, 2000.
[10] Q. Sun, X. G. Gong, Q. Q. Zheng, D. Y. Sun, G. H. Wang, *Phys. Rev. B* **1996**, *54*, 10896.
[11] Q. Sun, Q. Wang, J. Z. Yu, Z. Q. Li, J. T. Wang, Y. Kawazoe, *J. Phys. I* **1997**, *7*, 1233.
[12] A. Prince, G. V. Raynor, D. S. Evans, *Phase Diagrams of Ternary Gold Alloys*, The Institute of Metals, London, **1990**, p. 485.
[13] J. H. Schön, C. Kloc, B. Batlogg, *Nature* **2000**, *408*, 549.
[14] T. F. Fässler, *Angew. Chem.* **2001**, *113*, 4289; *Angew. Chem. Int. Ed.* **2001**, *40*, 4161.
[15] F. Weigend, M. Häser, *Theor. Chem. Acc.* **1997**, *97*, 331.
[16] F. Weigend, M. Häser, H. Patzelt, R. Ahlrichs, *Chem. Phys. Lett.* **1998**, *294*, 143.
[17] D. Andrae, U. Häussermann, M. Dolg, H. Stoll, H. Preuss, *Theor. Chim. Acta* **1990**, *77*, 123.
[18] A. W. Ehlers, M. Böhme, S. Dapprich, A. Gobbi, A. Höllwarth, V. Jonas, K. F. Köhler, R. Stegmann, A. Veldkamp, G. Frenking, *Chem. Phys. Lett.* **1993**, *208*, 111.
[19] P. Pyykkö, N. Runeberg, F. Mendizabal, *Chem. Eur. J.* **1997**, *3*, 1451.
[20] R. Ahlrichs, M. Bär, M. Häser, H. Horn, C. Kölmel, *Chem. Phys. Lett.* **1989**, *162*, 165.

Naked-Eye Sensitive Detection of Immunoglubulin G by Enlargement of Au Nanoparticles In Vitro**

Zhanfang Ma and Sen-Fang Sui*

Methods that enable the rapid, sensitive, accurate, and inexpensive detection of substances in a complex sample matrix are important tools. Immunoassays are based on the use of an antibody that reacts specifically with an antigen to be tested. The quantification of immunoassays is generally achieved by measuring the specific activity of a label, that is, its radioactivity, fluorescence, chemiluminescence, or bioluminescence. Because of its special properties which include ease of preparation, high density, large dielectric constant, and biocompatibility,[1] Au nanoparticles, as an amplification tag, have been the subject of research directed at gene analysis[2] and antibody or antigen detection.[3]

The observation of larger Au nanoparticles is beneficial. However, to increase the labeling efficiency, smaller Au nanoparticles are usually used to prepare the conjugate of the antibody or antigen and colloidal gold.[4] Particularly in histochemistry or cytochemistry, ultra-small Au nanoparticles ($\sim$1.5 nm) are essential.[5]

The sensitivity of the small immunogold particles is usually enhanced by silver staining.[6] While silver enhancement allows the signals from immunogold targeting to be seen on blots, their detecting concentration after silver staining can often reach a level of approximately a picogram per microliter ($pg\,\mu L^{-1}$).[7, 8] This is still much lower than that of fluorescent, radioactive, and enzyme-colorometric methods.[9] The lowest detecting concentration for silver staining is generally acknowledged to be 0.1 $pg\,\mu L^{-1}$.[10]

Herein we use a mixture of $HAuCl_4$ and $NH_2OH \cdot HCl$, instead of silver staining solution, to enlarge immunogold particles immobilized on the nitrocellulose strip, based on the seeding method[11] of detecting human immunoglubulin G (h-IgG) in vitro. Although silver enhancement is commonly used to visualize protein-, antibody-, and DNA-conjugated gold nanoparticles in histochemical electron microscopy studies,[4, 12] it has not been used for the enlargement of Au nanoparticles by $HAuCl_4$ and $NH_2OH \cdot HCl$ in vitro to enhance the detection of h-IgG by the naked eye. The detecting limit of the present method is significantly increased to approximately 10 $pg\,mL^{-1}$, thereby rivaling the limits of fluorescent, radioactive, and enzyme-colorometric methods.[9]

Figure 1 shows the principle behind the method used here. While NH_2OH is thermodynamically capable of reducing Au^{3+} ions to bulk metal,[13] the reaction is dramatically accelerated by Au surfaces.[14] As a result, no new particle

[*] Prof. S.-F. Sui, Dr. Z. Ma
Department of the Biological Sciences & Biotechnology
State-Key Laboratory of Biomembrane
Tsinghua University
Beijing 100084 (P. R. China)
Fax: (+86) 10-6278-4768
E-mail: suisf@mail.tsinghua.edu.cn

[**] This research was financed by grants from the National Natural Science Foundation of China (NSFC) and Tsinghua University.

  1433-7851/02/4112-2176 $ 20.00+.50/0

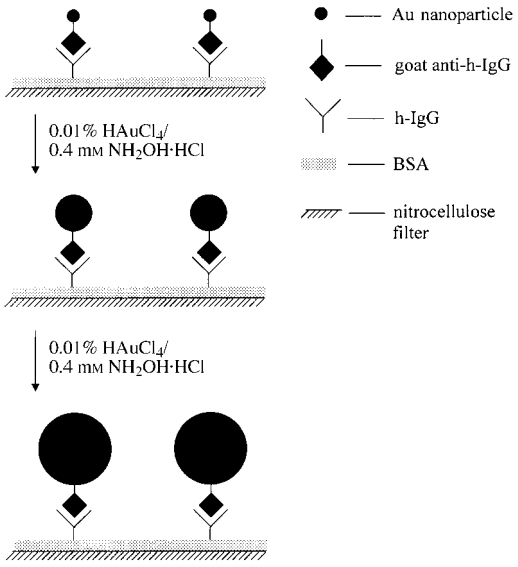

Figure 1. Schematic diagram of the immunodot assay improved by enlarging the Au nanoparticles with $HAuCl_4$ and $NH_2OH \cdot HCl$ in vitro; BSA = bovine serum albumin.

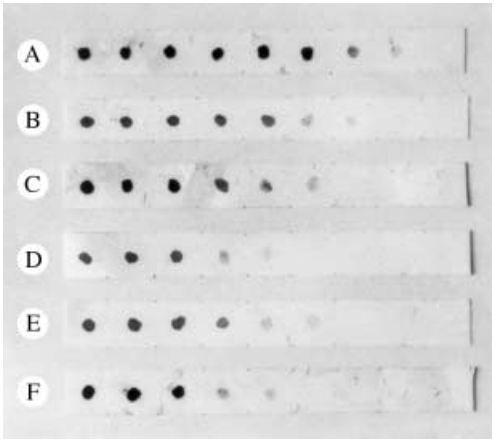

Figure 2. Immunoblot of dilutions of h-IgG detected with goat anti-h-IgG-$Au_{10\,nm}$. A 2 μL h-IgG dilution and buffer blank was applied to the nitrocellulose strips. They were then treated with 0.01 % $HAuCl_4$/0.4 mM $NH_2OH \cdot HCl$ twice (A) and once (B); with silver nitrate/hydroquinone twice (C) and once (D); and with silver acetate/hydroquinone twice (E) and once (F). The concentrations of h-IgG from left to right: 1×10^5, 4×10^4, 8×10^3, 2×10^3, 400, 300, 200, 10 pg mL^{-1}, and the buffer blank (solvent of h-IgG dilutions).

nucleation occurs in solution and all the added Au^{3+} ions go into the production of larger particles. The Au nanoparticles were immobilized on the nitrocellulose strips through the specific interaction between goat anti-h-IgG conjugated Au nanoparticles and target h-IgG preadsorbed on the nitrocellulose strips. These immobilized Au nanoparticles were enlarged by 0.01 % $HAuCl_4$ and 0.4 mM $NH_2OH \cdot HCl$. Consequently, the staining signals were considerably enhanced.

For silver staining, the detection efficiency of immunogold is closely related to the type of silver salt being used.[15] A number of silver salts, silver nitrate,[16] silver lactate,[17] and silver acetate,[18] have been used as the silver staining solution. We employed silver nitrate and silver acetate as the silver staining solution. The enlarging reaction is usually complete within 2 min,[11] therefore a time of 2 min was used for the mixture of 0.01 % $HAuCl_4$ and 0.4 mM $NH_2OH \cdot HCl$ enlargement step.

As shown in Figure 2, there is no detectable staining when the concentration of h-IgG is less than 10 and 200 pg mL^{-1}. This corresponds to the enlargement with the mixture of 0.01 % $HAuCl_4$ and 0.4 mM $NH_2OH \cdot HCl$ using double (Figure 2 A) and single staining (Figure 2 B), respectively. This result indicates that the detection limits are significantly increased to 10 and 200 pg mL^{-1}. The signals for the controls using just the solvent used for the h-IgG dilutions (20 mM Tris-HCl buffer pH 7.4, 0.15 M NaCl; Tris = tris(hydroxymethyl)-aminomethane) instead of h-IgG dilutions (Figure 2 A and B) are negative. In contrast, for silver staining with the mixture of silver nitrate and hydroquione for 30 min each in a dark room, no detectable staining can be observed when the concentration of h-IgG is less than 300 and 400 pg mL^{-1}. This concentration corresponds to the double and single staining and indicates that the detection limit is 300 pg mL^{-1} (Figure 2 C) and 400 pg mL^{-1} (Figure 2 D). Silver acetate staining gave similar results (Figure 2 E and F).

To examine the benefits of enhancing sensitivity, 10 nm Au nanoparticles (as seeds in aqueous solution) were used to study the increase of the surface area of the Au nanoparticles induced by the enlargement with 0.01 % $HAuCl_4$ and 0.4 mM $NH_2OH \cdot HCl$. The diameters of the Au nanoparticles were increased to around 60 nm and 200 nm after single and double enlargement, respectively (Figure 3). Compared with the surface areas of 10 nm Au nanoparticles without enlargement, these results mean that the surface areas of the Au nanoparticles were remarkably increased approximately 36-fold and 400-fold.

Possibly, some free Au nanoparticles exist in the conjugate of goat anti-h-IgG-$Au_{10\,nm}$. To address the nonspecific adsorption of the free Au nanoparticles on the nitrocellulose strips control experiments were performed. A 2 μL 20 mM Tris-HCl buffer (pH 7.4, 0.15 M NaCl) and a 2 μL 10 pg mL^{-1} h-IgG dilution were spotted on the nitrocellulose strips. Some of these strips were blocked with 3 % bovine serum albumin (BSA). The strips were then incubated in the free colloidal gold (10 nm) solution. The optical density $OD_{516\,nm}$ of the colloidal gold was the same as that of the conjugate of goat anti-h-IgG-$Au_{10\,nm}$. The nitrocellulose strips were treated with the mixture of 0.01 % $HAuCl_4$ and 0.4 mM $NH_2OH \cdot HCl$ for 2 min each time at 30 °C, rinsed with water, and then treated with fresh solution for another 2 min at 30 °C. Detectable staining caused by the nonspecific adsorption of free Au nanoparicles could not be observed (Figure 4). For the nitrocellulose strips without the 3 % BSA blocking, the background was very noticeable (Figure 4 B) which implies that the free Au nanoparicles were substantially adsorbed on the nitrocellulose strips. In contrast, for the nitrocellulose strips with the 3 % BSA blocking the background was fairly pale (Figure 4 A). This result suggests that 3 % BSA can effectively block the nonspecific adsorption of the free Au nanoparticles. These results demonstrate that neither nonspecific binding of gold nanoparticles nor nonspecific new gold nucleation formed onto the surface of nitrocellulose strips blocked with BSA.

  1433-7851/02/4112-2177 $ 20.00+.50/0

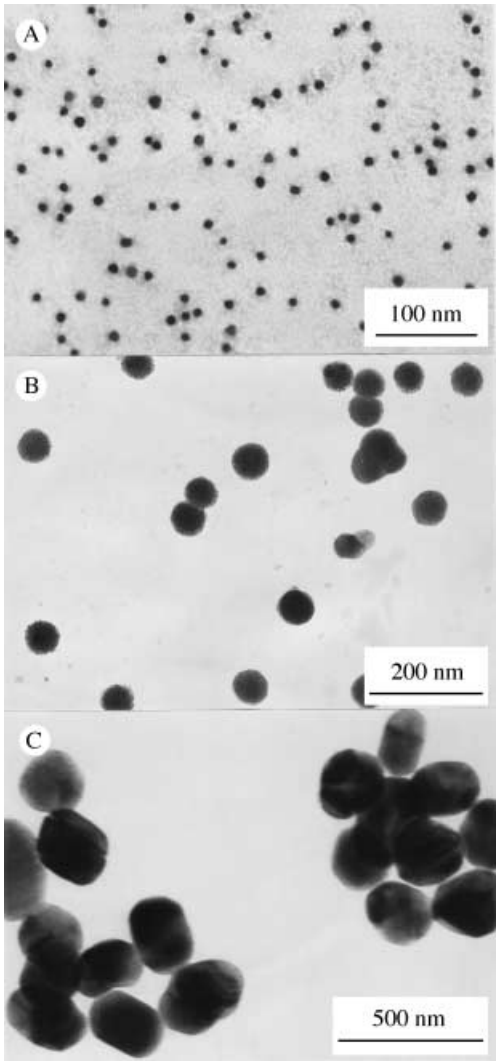

Figure 3. TEM images of Au nanoparticles enlarged by 0.01 % $HAuCl_4$ and 0.4 mM $NH_2OH \cdot HCl$ in aqueous solution. A) Seeds, B) after one treatment for 2 min, C) after two treatments each of 2 min.

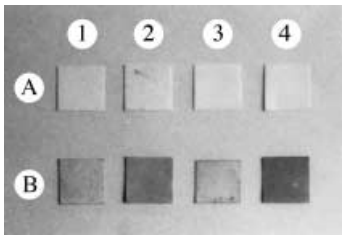

Figure 4. Effect of BSA blocking on the nonspecific adsorption of free Au nanoparticles. 2 μL 20 mM Tris-HCl buffer (pH 7.4, 0.15 M NaCl; 1 and 2) and 10 pg mL^{-1} h-IgG dilution (3 and 4) spotted onto nitrocellulose strips. These strips were incubated in a solution without Au nanoparticle and treated once (1 and 3) or twice (2 and 4) with 0.01 % $HAuCl_4$ and 0.4 mM $NH_2OH \cdot HCl$. The strips in part A were blocked while those in part B were not blocked.

In summary, enlarging Au nanoparticles immobilized on nitrocellulose strips was performed with the mixture of 0.01 % $HAuCl_4$ and 0.4 mM $NH_2OH \cdot HCl$ instead of silver staining to detect h-IgG in vitro, as a result the detection sensitivity was significantly increased to approximately 10 pg mL^{-1}. This level rivals the limits of fluorescent, radioactive, enzyme-colorometric, and chemiluminent methods. The method described is simple, rapid, economic, sensitive, specific, and is suitable for detection with the naked eye. Further experiments to understand the difference in mechanisms between the Au method and silver staining and also to compare the present method with other techniques are still underway, however, these current results suggest a new way in immunoassay.

Experimental Section

Conjugate of goat anti-h-IgG-$Au_{10\,nm}$ and h-IgG were obtained from the Xinjingke Biotechnology Company (Beijing, China). Hydrochloroauric acid ($HAuCl_4 \cdot 4H_2O$, [14-1]), hydroxylamine hydrochloride ($NH_2OH \cdot HCl$, [59-11]), silver nitrate ($AgNO_3$, [33-2]), silver acetate (AgAc, [33-61]), hydroquinone [62-4], sodium thiosulfate pentahydrate ($Na_2S_2O_3 \cdot 5H_2O$, [24-25]), aluminum potassium sulfate dodecahydrate ($KAl(SO_4)_2 \cdot 12H_2O$, [68-9]), and boric acid (H_3BO_3, [1-20]) were purchased from Beijing Chemical Reagents Company (Beijing, China, [product number]). BSA, gelatin, and Tris base were obtained from Sigma (USA). Water used in the study was Milli-Q water (18 MΩ cm^{-1}). h-IgG was diluted with 20 mM Tris-HCl buffer (pH 7.4, 0.15 M NaCl). A 2 μL of h-IgG dilutions with different concentrations were spotted on the dry nitrocellulose strips (Hybond-C, 0.45 μm; Amersham, Buckinghamshire, UK). The nitrocellulose strips were held in a dry-air thermostat at 60 °C for 1 h. The strips, after spotting, were incubated for 1 h at 37 °C in a blocking buffer (20 mM Tris-HCl, pH 7.4, 0.15 M NaCl) of 3 % BSA. The strips were then incubated in solutions of the conjugate of goat anti-h-IgG-$Au_{10\,nm}$ for 2 h at 37 °C. The strips were then fully washed with 20 mM Tris-HCl buffer (pH 7.4, 0.15 M NaCl) and Milli-Q water. Next, some strips were treated with 0.01 % $HAuCl_4$ and 0.4 mM $NH_2OH \cdot HCl$ (pH 6.0) for 2 min at 30 °C, rinsed, and then treated for two more minutes. Other strips were treated in a darkroom with silver nitrate developer (20 mM $AgNO_3$, 50 mM hydroquinone, 0.1 % gelatin, pH 3.5 citrate acid buffer), or with silver acetate developer (20 mM AgAc, 50 mM hydroquinone, 0.1 % gelatin, pH 3.5 citrate acid buffer) for 30 min at 30 °C. Some of these strips were rinsed with water and again treated with fresh silver nitrate or silver acetate developer for 30 minutes more. For the gold treatment, $NH_2OH \cdot HCl$ solution was incubated with the strips immediately after they had been incubated with 0.01 % $HAuCl_4$. For the silver treatment, hydroquinone was added to each silver developer just prior to use. A common fixer (25 % $Na_2S_2O_3$, 1.2 % $KAl(SO_4)_2$, 1.5 % Na_2SO_3, 1 % H_3BO_3, and 1 % HAc) was used for 1 min to stop the amplification prior to Milli-Q water washes. $HAuCl_4$, $NH_2OH \cdot HCl$, $AgNO_3$, and AgAc solutions were freshly prepared in a lightproof container. Only thoroughly precleaned glassware was used to prepare all of the solutions used; the removal of the dust was required from all of the materials used in the study.

Received: September 17, 2001
Revised: January 4, 2002 [Z17916]

[1] L. A. Lyon, M. D. Musick, P. C. Smith, B. D. Reiss, D. J. Pena, M. J. Natan, *Sens. Actuators*, *B* **1999**, *54*, 110 – 124.
[2] a) T. A. Taton, C. A. Mirkin, R. L. Letsinger, *Science* **2000**, *289*, 1757 – 1759; b) B. Dubertret, M. Calame, A. J. Libchaber, *Nat. Biotechnol.* **2001**, *19*, 365 – 370; c) S.-J. Park, A. A. Lazarides, C. A. Mirkin, P. W. Brazis, C. R. Kannewurf, R. L. Letsinger, *Angew. Chem.* **2000**, *112*, 4003 – 4006; *Angew. Chem. Int. Ed.* **2000**, *39*, 3845 – 3848; d) L. He, M. D. Music, S. R. Nicewarner, F. G. Salinas, S. J. Benkovic, M. J. Natan, C. D. Keating, *J. Am. Chem. Soc.* **2000**, *122*, 9071 – 9077; e) J. E. Geswicki, L. E. Strong, L. L. Kiessling, *Angew. Chem.* **2000**, *112*, 4741 – 4744; *Angew. Chem. Int. Ed.* **2000**, *39*, 4567 – 4570.
[3] K. R. Brown, A. P. Fox, M. J. Natan, *J. Am. Chem. Soc.* **1996**, *118*, 1154 – 1157.
[4] M. A. Hayat, *Colloid Gold: Principles, Methods and Applications*, *Vol. 1*, Academic Press, San Diego, **1989**.
[5] J. M. Robinson, T. Takizawa, D. D. Vandre, *J. Microsc.* **2000**, *199*, 163 – 179.

  1433-7851/02/4112-2178 $ 20.00+.50/0

[6] *Immunogold-Silver Staining: Principles, Methods and Applications* (Ed.: M. A. Hayat), Academic Press, New York, **1995**.
[7] a) P. Eliades, E. Karagouni, I. Stergiaton, K. Kiras, *J. Immunol. Methods* **1998**, *210*, 123 – 132; b) G. Mayer, R. D. Leone, J. F. Hainfeld, M. Bendayan, *J. Histochem. Cytochem.* **2000**, *48*, 464 – 469.
[8] M. G. Sumi, A. Mathai, C. Sarada, V. V. Radhakrishnan, *J. Clin. Microbiol.* **1999**, *37*, 3925 – 3927.
[9] a) V. A. J. Kempf, K. Trebesius, I. B. Autenrieth, *J. Clin. Microbiol.* **2000**, *38*, 830 – 838; b) P. Kite, B. M. Dobbins, M. H. Wilcox, M. J. McMahon, *Lancet* **1999**, *354*, 1504 – 1507; c) P. V. Coyloe, A. Desai, D. Wyatt, C. McCaughey, H. E. O'Neil, *J. Virol. Methods* **1999**, *83*, 75 – 82.
[10] J. F. Hainfeld, F. R. Furuya, *Immunogold-Silver Staining: Principles, Methods and Applications*, (Ed.: M. A. Hayat), Academic Press, New York, **1995**, p. 92.
[11] K. R. Brown, M. J. Natan, *Langmuir* **1998**, *14*, 726 – 728.
[12] R. Rufner, N. E. Carson, M. Forte, G. Danscher, J. Gu, G. W. Hacker, *Cell Vision* **1995**, *2*, 327 – 333.
[13] $E = 1$ V versus NHE(Au) and $E_{1/2} = -0.4$ V versus NHE(NH_2OH); NHE = normal hydrogen electrode. A. J. Bard, *Encyclopedia of Electrochemistry of the Elements*, *Vol. 4*, Marcel Dekker, New York, **1975**.
[14] H. Perrot, J. R. Martin, P. J. Clechet, *J. Electrochem. Soc.* **1988**, *135*, 2881 – 2885.
[15] G. W. Hacker, G. Danscher, L. Grimelius, C. Hauser-Kronberger, W. H. Muss, A. Schiechl, J. Gu, O. Dietze. *Immunogold-Silver Staining: Principles, Methods and Applications*, (Ed.: M. A. Hayat), Academic Press, New York, **1995**, p. 29.
[16] T. Krenács, E. Molnár, E. Dobó, L. Dux, *Histochem. J.* **1989**, *21*, 145.
[17] a) G. Danscher, *Histochemistry* **1981**, *71*, 1 – 16; b) G. Danscher, *Histochemistry* **1981**, *71*, 81 – 88.
[18] G. W. Hacker, L. Grimelius, G. Danscher, G. Bernatzky, W. Muss, H. Adam, J. Thurner, *J. Histotechnol.* **1988**, *11*, 213 – 221.

Ligand Topology Tuning of Iron-Catalyzed Hydrocarbon Oxidations**

Miquel Costas and Lawrence Que, Jr.*

Nature has evolved a number of nonheme iron oxygenases capable of the stereoselective oxidation of C–H and C=C bonds.[1, 2] Still far from being understood are the factors that control the ability of iron centers to catalyze a range of reactions such as alkane hydroxylation, olefin epoxidation, and olefin *cis*-dihydroxylation. In our effort to develop bio-inspired nonheme iron catalysts, we have discovered a family of iron complexes with tetradentate pyridine/amine ligands that, in combination with H_2O_2, are capable of carrying out the above transformations with high stereoselectivity.[3–7] Enantioselectivity has also been obtained with the chiral ligand *N*,*N*′-bis(2-pyridylmethyl)-*N*,*N*′-dimethyl-*trans*-1,2-diaminocyclohexane (bpmcn).[8] A priori, tetradentate ligands with this type of architecture can adopt three different topologies (Scheme 1).[9–11] While Schiff's base ligands (e.g. salen) often afford complexes with the *trans* or planar

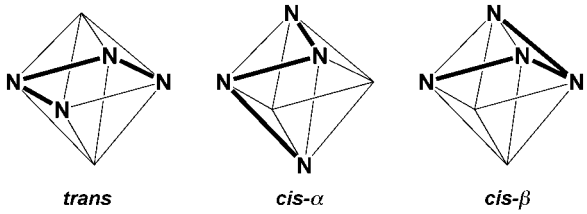

Scheme 1. Three different topologies that can be adopted by tetradentate ligands such as *N*,*N*′-bis(2-pyridylmethyl)-*N*,*N*′-dimethyl-*trans*-1,2-diaminocyclohexane (bpmcn).

topology, ligands such as bpmcn in which the imine functionalities have been reduced give rise to complexes with *cis*-α and/or *cis*-β topologies. We have undertaken a series of systematic studies to uncover the factors that control the catalytic reactivity of the nonheme iron center in this family of complexes.[5–7] Herein we report the unexpectedly distinct oxidation behavior of two [Fe^{II}(bpmcn)] catalysts, whose structures differ only by their ligand topologies.

[Fe^{II}(bpmcn)($OTf)_2$] (**1**, OTf = trifluoromethanesulfonate) complexes in both *cis*-α and *cis*-β ligand topologies can be synthesized by independent routes, and the structures of α-**1** and the related β-[Fe^{II}(5-Me_2-bpmcn)($OTf)_2$] have recently been established by crystallography.[8, 12] The NMR spectra of the two complexes strongly suggest that they each retain their respective ligand topologies in solution (Figure 1). Complex

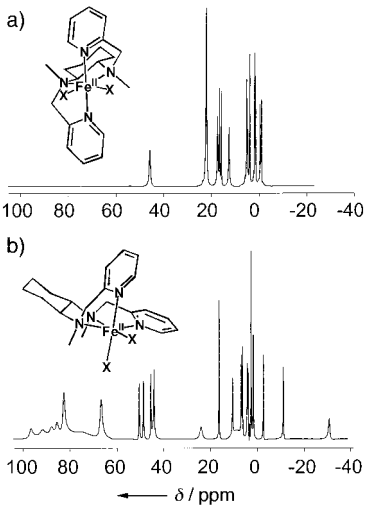

Figure 1. ^{1}H NMR spectra of α-[Fe^{II}(bpmcn)($CD_3CN)_2$]$^{2+}$ (a) and β-[Fe^{II}(bpmcn)($CD_3CN)_2$]$^{2+}$ (b) in CD_3CN solution at ambient temperature.

α-**1** exhibits 12 paramagnetically shifted signals, as expected for a C_2-symmetric high-spin Fe^{II} complex, while the β isomer shows 24 resonances. These isomers do not interconvert even after heating solutions of either isomer in acetonitrile at 50 °C for one day. The high barrier to interconversion arises from the fact that the N-methyl groups of the ligand have distinct

[*] Prof. Dr. L. Que, Jr., Dr. M. Costas
Department of Chemistry
and Center for Metals in Biocatalysis
University of Minnesota
207 Pleasant Street SE, Minneapolis, MN 55455 (USA)
Fax: (+1) 612-624-7029
E-mail: que@chem.umn.edu

[**] We thank the National Institutes of Health for financial support (GM33162 to L.Q.) and Fundacio La Caixa for a postdoctoral fellowship (M.C.).

  1433-7851/02/4112-2179 $ 20.00+.50/0